Original Article

Avicenna Journal of Medical Biotechnology
Volume 13, Issue no. 2, 58-64
http://dx.doi.org/10.18502/ajmb.v13i2.5519

Check for updates

Designing and Development of a Tandem Bivalent Nanobody against $VEGF_{165}$

Farnaz Khodabakhsh [1], Morteza Salimian [2], Pardis Ziaee [3], Fatemeh Kazemi-Lomedasht [4], Mahdi Behdani [4], and Reza Ahangari Cohan [5*]

1. Department of Genetics and Advanced Medical Technology, Medical Biotechnology Research Center, Faculty of Medicine, AJA University of Medical Sciences, Tehran, Iran
2. Department of Medical Laboratory, Kashan University of Medical Sciences, Kashan, Iran
3. Department of Biology, Central Tehran Branch, Islamic Azad University, Tehran, Iran
4. Venom and Biotherapeutics Molecules Laboratory, Department of Biotechnology, Biotechnology Research Center, Pasteur Institute of Iran, Tehran, Iran
5. Department of Nanobiotechnology, New Technologies Research Group, Pasteur Institute of Iran, Tehran, Iran

Abstract

Background: Inhibition of angiogenesis using monoclonal antibodies is an effective strategy in cancer therapy. However, they could not penetrate sufficiently into solid tumors. Antibody fragments have solved this issue. However, they suffer from short in vivo half-life. In the current study, a tandem bivalent strategy was used to enhance the pharmacokinetic parameters of an anti-VEGF165 nanobody.

Methods: Homology modeling and MD simulation were used to check the stability of protein. The cDNA was cloned into pHEN6C vector and the expression was investigated in WK6 *Escherichia coli* (*E. coli*) cells by SDS-PAGE and western blot. After purification, the size distribution of tandem bivalent nanobody was investigated by dynamic light scattering. Moreover, *in vitro* antiproliferative activity and pharmacokinetic study were studied in HUVECs and Balb/c mice, respectively.

Results: RMSD analysis revealed the tandem bivalent nanobody had good structural stability after 50 *ns* of simulation. A hinge region of llama IgG2 was used to fuse the domains. The expression was induced by 1 *mM* IPTG at 25 *°C* for overnight. A 30 *kDa* band in 12% polyacrylamide gel and nitrocellulose paper has confirmed the expression. The protein was successfully purified using metal affinity chromatography. MTT assay revealed there is no significant difference between the antiproliferative activity of tandem bivalent nanobody and the native protein. The hydrodynamic radius and terminal half-life of tandem bivalent nanobody increased approximately 2-fold by multivalency compared to the native protein.

Conclusion: Our data revealed that the physicochemical as well as *in vivo* pharmacokinetic parameters of tandem bivalent nanobody was significantly improved.

Avicenna J Med Biotech 2021; 13(2): 58-64

Keywords: Cancer, Pharmacokinetics, Single domain antibody, Vascular endothelial growth factor

*** Corresponding author:**
Reza Ahangari Cohan, Ph.D., Department of Nanobiotechnology, New Technologies Research Group, Pasteur Institute of Iran, Tehran, Iran
Tel: +98 21 64112168
Fax: +98 21 6646513
E-mail: cohan_r@pasteur.ac.ir
Received: 17 Aug 2020
Accepted: 7 Nov 2020

Introduction

Approximately 30% of recombinant DNA technology based drugs are antibodies that are frequently used in inflammatory diseases and cancers [1,2]. Monoclonal antibodies (mAbs) could concurrently be used for diagnostic and therapeutic purposes in medicine. However, their manufacturing is practically difficult and costly and puts an extra burden on healthcare system. In addition, because of the large size (~150 *kDa*), they have a poor distribution and low penetration rate into the solid tumors [3]. Therefore, many efforts have been made to overcome such limitations and improve the pharmacological properties including design of antigen-binding fragments (Fab), variable fragments (Fv), single-chain variable Fragments (scFv), and single-domain antibodies (Nanobodies) [4,5]. Antibody fragments have superior advantages over conventional antibodies. For example, due to the smaller size, they penetrate easily to solid tissues. Moreover, the lack of Fc domain reduces the risk of immunogenicity in humans as well as heterogeneity in the product. In the

manufacturing process, they do not need mammalian expression systems which are often costly and time-consuming [6]. Prokaryotic expression systems can be applied to manufacture them and usually provide much more protein than eukaryotic systems [7]. Due to high solubility, low cost of production, high stability at harsh conditions, rapid penetration into solid tissues, detection of hidden antigenic sites, and lower immunogenicity with a specific affinity, the smallest binding antibody fragments (Nanobodies) have more advantages than other antibody fragments [4,8]. However, they suffer from short *in vivo* half-life and low affinity [9]. Numerous strategies were developed for enhancing pharmacokinetic parameters of small therapeutic proteins such as PEGylation and PASylation [10-14]. However, each strategy has its own cons and pros. For example, PASylation technique suffers from low expression level of PASylated protein due to repeat sequences as observed in our previous study [14]. Moreover, in another study, it was elucidated that the PAS sequence could decrease the affinity of PASylated protein in comparison to the native one [15]. The preparation of multivalent forms of antibody fragments enhances the efficacy and *in vivo* distribution [16]. Increasing the valency of antibody derivatives improves the pharmacokinetic properties of these fragments as well [1,17]. In addition, by repeating monovalent single domain antibodies, the binding avidity could increase compared to the monomeric form [16].

Since Vascular Endothelial Growth Factor$_{165}$ (VEG F$_{165}$) isoform is a key factor in tumor angiogenesis and metastasis [18], therefore, in the current study, a recombinant tandem bivalent single-domain antibody against VEGF$_{165}$ was designed, expressed, and purified. Finally, the size distribution and *in vivo* half-life of purified protein were investigated.

Materials and Methods

3D-modeling and molecular dynamics simulation

The 3D-structure of tandem bivalent nanobody was generated using homology modeling. The crystal structure of nanobody NbFedF9 (PDB code: 4W6Y, 1.57 Å) was used as the template. One hundred models were generated by Modeller software version 9.24 [19]. The best model was selected based on discrete optimized protein energy (DOPE) score. The quality of the model was assessed by phi (φ) and psi (ψ) analysis [20]. The stability of tandem bivalent nanobody was finally investigated by all-atom molecular dynamics simulation using GROMACS package version 2016.3 with OPLS-AA forcefield in a Linux Mint 17 operating system [21]. The Extended Simple Point Charge (SPCE) water model was used for the solvent molecules. Tandem bivalent nanobody was solvated in a cubic box at a distance of 1 *nm* from the edges. The periodic boundary conditions were also applied. Appropriate number of Na^+ and Cl^- ions were added to neutralize the system. The steepest descent algorithm was used for energy minimization of the system within 200 *picoseconds*. The temperature and pressure of system were kept at 300 *K* and 1 *atmosphere* using Berendsen thermostat and Parrinello-Rahman barostat algorithms, respectively. The system was then subjected to the all-atom simulation until the Root Mean Square Deviation (RMSD) of the fusion protein reached to a plateau. All visualizations were performed using VMD software version 1.9.3 [22].

Construct design and cloning

The anti-VEGF$_{165}$ specific nanobody gene was a gift from Dr. Behdani (Pasteur Institute of Iran) and subcloned into pHEN6C vector. The nanobody gene was amplified using forward (5´-GCCCAG CCG GCC ATG GCC CAG KTG CAG CTA CAG GAG TCN GGN GG-3´) and reverse (5´-GCC TGA TTC CTG CAG CTG CAC CTG TGC CAT TGG AGC TTT GGG AGC TTT GGA GCT GGG GTC TTC GCT GTG GTG CGC TGA GGA GAC GGT GAC CTG GGT-3´) primers. The PCR program was as follows: initial denaturation at 95°*C* for 10 *min*, followed by 30 cycles of denaturation at 95°*C* for 40 *s*, annealing at 60°*C* for 40 *s*, extension at 72°*C* for 40 *s*, and final elongation at 72°*C* for 10 *min*. After the PCR purification, the product was digested with *Pst*I and *Sfi*I restriction enzymes and ligated into pHEN6C vector that comprises the first anti-VEGF$_{165}$ nanobody [9]. The accuracy of recombinant construct (VEGF$_{165}$-tandem bivalent nanobody) was confirmed by sequencing.

Expression

Transformation of the recombinant plasmid to week 6 *E. coli* cells was performed by heat shock method. The cells were cultured on Luria–Bertani (LB) agar plates with 100 *µg/ml* of ampicillin and incubated overnight at 37°*C*. The colonies were then inoculated into 5 *ml* of Terrific Broth (TB) medium in a shaker incubator at 37°*C* until the OD$_{600}$ reached to 0.5. The expression was induced by adding 1 *mM* of Isopropyl ß-D-1-thiogalactopyranoside (IPTG) to the culture after 16 *hr*. Finally, the cells were centrifuged at 4000 *g* for 5 *min* and the obtained pellets were stored at -20°*C* for further steps.

SDS-PAGE and western blotting

SDS–PAGE was done in a 12% (*w/v*) gel with a Bio-Rad instrument according to the manufacturer's protocol (Bio-Rad, USA). The protein samples were mixed with the loading buffer and boiled at 95°*C* for 5 *min* and subsequently subjected to electrophoresis. The staining of gel was done using Coomassie Brilliant Blue G-250. The gel was destained using 2.5% methanol and 10% acetic acid for 4 *hr*. To identify the desired protein, a western blot technique was employed using anti-His monoclonal antibody. The separated proteins were transferred onto a nitrocellulose membrane (Sigma, USA). Then, blocking step was performed using 2% skim milk in PBS. The specific detection of the desired protein was carried out by an

anti-His HRP conjugated antibody (1:2000 dilution, Roche, USA). The color development for peroxidase activity was performed by DAB solution (60 *mg* of DAB, 100 *µl* of H_2O_2, 6 *ml* of methanol, and 50 *ml* of TBS up to 100 *ml* of ultra-pure water) (Sigma, USA).

Protein extraction and purification

For purification, the bacterial cultures were scaled up to 750 *ml* in a shaker incubator at 37°*C*. When the OD_{600} of cultures reached to 0.5, the induction was done with 1 *Mm* of IPTG and they were incubated for 16 *hr*. After harvesting the cells, the periplasmic proteins were extracted from the pellets by the osmotic method [10]. The nickel-nitrilotriacetic acid (Qiagen, USA) affinity chromatography was used for purification of the periplasmic extracts. The washing step was done using 20 *mM* of imidazole, and then, the desired protein was eluted with 500 *mM* of imidazole. The purified protein was also analyzed using 12% gel polyacrylamide electrophoresis. The protein was concentrated and buffer exchanged using Amicon® ultrafilter (MWCO 3 *kDa*, Millipore, USA) for further characterizations. Additionally, the native protein was expressed and purified as control with the same procedures in the current study.

Size distribution measurements

Size distributions of tandem bivalent anti-$VEGF_{165}$ nanobody and anti-$VEGF_{165}$ nanobody were measured using Zetasizer Nano ZS (Malvern, USA) at concentration of 0.3 *mg/ml*.

Proliferation assay

The antiproliferative effect of nanobody and tandem bivalent nanobody was studied *in vitro*. HUVEC (Lonza Biologics, USA) and HEK293 (Pasteur Institute of Iran) cells were used as VEGFR2-positive [23] and -negative [24] cells, respectively. The cells were cultured in the specific media according to the instructions. Different concentrations of proteins were mixed with recombinant $VEGF_{165}$ (50 *ng/ml*) for 4 *hr* and the mixture was then added to the cultured cells. After 72 *hr* of incubation, 50 *µl* of MTT solution (5 *mg/ml*) was added and the plates were incubated for 4 *hr* at 37°*C*. Finally, DMSO was added to the wells and the absorbance was measured at a wavelength of 570 *nm* using Epoch spectrophotometer (BioTeK, USA). Two-way analysis of variance (ANOVA) was used to compare the significant difference ($p<0.05$) between the groups using Prism 8 (GraphPad Software, Inc., La Jolla, CA).

Pharmacokinetic study

Balb/c mice (18 *g*, n=18) were used for pharmacokinetic study. An intravenous dose (5 *mg/kg*) was injected to each mouse. Blood samples were collected at different time intervals (0, 15 *min*, 30 *min*, 1 *hr*, 2 *hr*, 3 *hr*, 4 *hr*, 5 *hr*, and 6 *hr*). PBS was used as negative control. After plasma preparation, the protein concentration was measured by a home-made ELISA using anti-His monoclonal antibody as previously described [16]. The terminal half-life ($T_{1/2}$) and Clearance (CL) were determined using linear regression of the last three plasma concentrations.

Results

3D-modeling and molecular dynamics simulation

Homology modeling and molecular dynamics simulation were used to check the stability of three dimensional structure of tandem bivalent nanobody. The crystal structure of nanobody NbFedF9 with a sequence identity of 72.1% was used for homology modeling. Ramachandran plot analysis (Phi and psi torsion angles) elucidated that 96.8% of residues were located in favored and allowed regions in the generated 3D-model. The RMSD analysis revealed that the 3D-model of fusion protein was stable after ~20 *nanoseconds* of molecular dynamics simulation in water (Figure 1).

Construct design and cloning

The nanobody gene was amplified using the primers from pHEN6-anti-$VEGF_{165}$ nanobody plasmid. The PCR product was purified, digested with *Pst*I and *Sfi*I restriction enzymes, and ligated into pHEN6C expression vector to construct the tandem bivalent nanobody (Figure 2). DNA sequencing confirmed the accuracy of the nanobody (S1, supplementary file) and tandem bivalent nanobody (S2, supplementary file) constructs.

SDS-PAGE and western blotting

SDS-poly acrylamide gel electrophoresis showed a band at ~30 *kDa* in the 12% gel (Figure 3). The western blot also confirmed the expression of recombinant anti-$VEGF_{165}$ tandem bivalent nanobody (Figure 4).

Protein extraction and purification

The nanobody and bivalent nanobody were extracted from the periplasmic space by the osmotic method and subjected to nickel affinity chromatography. Both

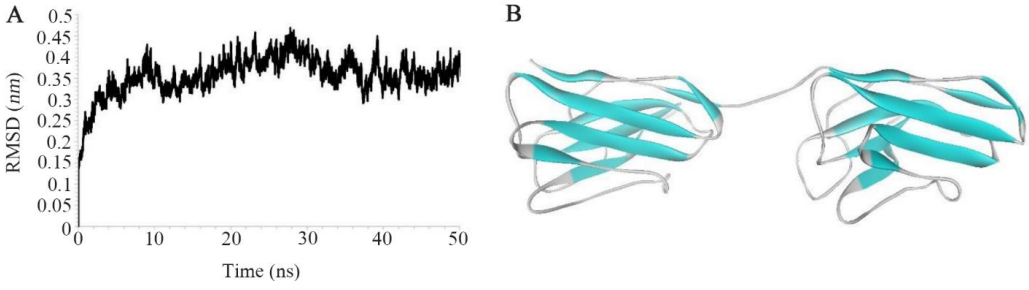

Figure 1. A) The root mean square deviations of tandem bivalent nanobody structure during 50 *nanoseconds* of molecular dynamics simulation. The fusion protein was reached to a plateau after ~20 *nanoseconds* of simulation in water. B) The 3D-structure of the designed tandem bivalent nanobody after 50 *nanoseconds* of molecular dynamics simulation.

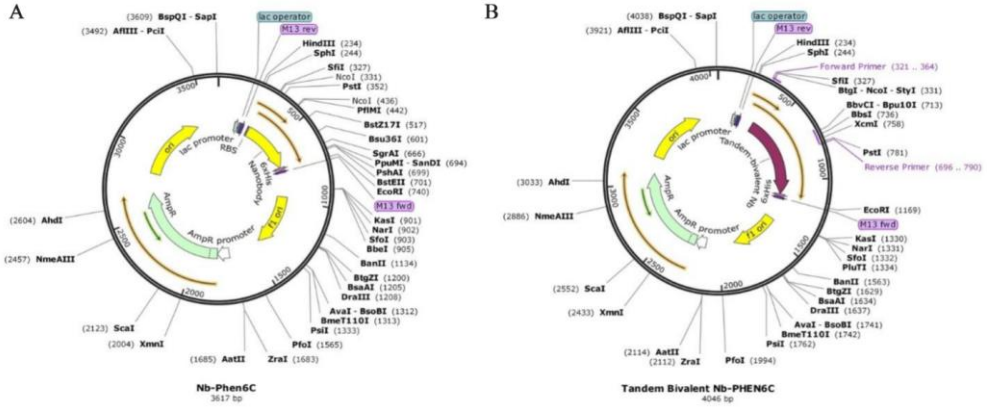

Figure 2. Schematic representation of (A) pHEN6-anti-VEGF$_{165}$ nanobody and (B) pHEN6c-VEGF$_{165}$-bivalent plasmids.

S1, supplementary file. > Nanobody

ATGAAATACCTATTGCCTACGGCAGCCGCTGGATTGTTATTA
CTCGCGGCCCAGCCGGCCATGGCCCAGGTGCAGCTGCAGGA
GTCTGGAGGAGGCTCGGTGCAGGCTGGAGGGTCTCTGAGAC
TCTCCTGTGCAGCCTCTGGATTCGCCTACAGTACCTACTCCA
TGGGCTGGTTCCGCCAGGTTCCAGGGAAGGAGCGTGAGGCG
GTCGCAACTATCAACAGTGGTACTTTTAGGCTATGGTATACA
GACTCAGTGAAGGGCCGATTCACCATCTCACGAGACAACGC
CAAGAACATGCTGTATCTGCAAATGAACAGCCTGAAACCTG
AGGACACGGCCATCTATTACTGTGCGGCGAGGGCCTGGTCC
CCCTATAGTTCGACTGTAGACGCCGGTGACTTTCGTTACTGG
GGCCAGGGGACCCAGGTCACCGTCTCCTCACACCACCATCA
CCATCACTAA

S2, supplementary file. > Tandem bivalent nanobody

ATGAAATACCTATTGCCTACGGCAGCCGCTGGATTGTTATTA
CTCGCGGCCCAGCCGGCCATGGCCCAGGTGCAGCTGCAGGA
GTCTGGAGGAGGCTCGGTGCAGGCTGGAGGGTCTCTGAGAC
TCTCCTGTGCAGCCTCTGGATTCGCCTACAGTACCTACTCCA
TGGGCTGGTTCCGCCAGGTTCCAGGGAAGGAGCGTGAGGCG
GTCGCAACTATCAACAGTGGTACTTTTAGGCTATGGTATACA
GACTCAGTGAAGGGCCGATTCACCATCTCACGAGACAACGC
CAAGAACATGCTGTATCTGCAAATGAACAGCCTGAAACCTG
AGGACACGGCCATCTATTACTGTGCGGCGAGGGCCTGGTCC
CCCTATAGTTCGACTGTAGACGCCGGTGACTTTCGTTACTGG
GGCCAGGGGACCCAGGTCACCGTCTCCTCAGCGCACCACAG
CGAAGACCCCAGCTCCAAAGCTCCCAAAGCTCCAATGGCCC
AGGTGCAGCTGCAGGAGTCTGGAGGAGGCTCGGTGCAGGCT
GGAGGGTCTCTGAGACTCTCCTGTGCAGCCTCTGGATTCGCC
TACAGTACCTACTCCATGGGCTGGTTCCGCCAGGTTCCAGGG
AAGGAGCGTGAGGCGGTCGCAACTATCAACAGTGGTACTTT
TAGGCTATGGTATACAGACTCAGTGAAGGGCCGATTCACCA
TCTCACGAGACAACGCCAAGAACATGCTGTATCTGCAAATG
AACAGCCTGAAACCTGAGGACACGGCCATCTATTACTGTGC
GGCGAGGGCCTGGTCCCCCTATAGTTCGACTGTAGACGCCG
GTGACTTTCGTTACTGGGGCCAGGGGACCCAGGTCACCGTC
TCCTCACACCACCATCACCATCACTAA

proteins were successfully eluted using buffer containing 500 *mM* of imidazole. The bivalent protein showed a band at ~30 *kDa* in 12% SDS-PAGE gel (Figure 5). However, the native protein showed a band at ~15 *kDa* in the 12% SDS-PAGE gel (Figure 6). The proteins were finally concentrated and buffer exchanged.

Size distribution

The hydrodynamic radius of tandem bivalent anti-VEGF$_{165}$ and anti-VEGF$_{165}$ nanobodies was investigated by Dynamic Light Scattering (DLS). The hydrodynamic radius of tandem bivalent anti-VEGF$_{165}$ nanobody increased approximately 2-fold by multivalency compared to anti-VEGF$_{165}$ nanobody (Figure 7). Size distribution showed a peak at 153 *nm* for tandem bivalent anti-VEGF$_{165}$ nanobody, while this value was 77 *nm* for anti-VEGF$_{165}$ nanobody [14]. Size distribution parameters of nanobody and tandem bivalent nanobody are summarized in table 1.

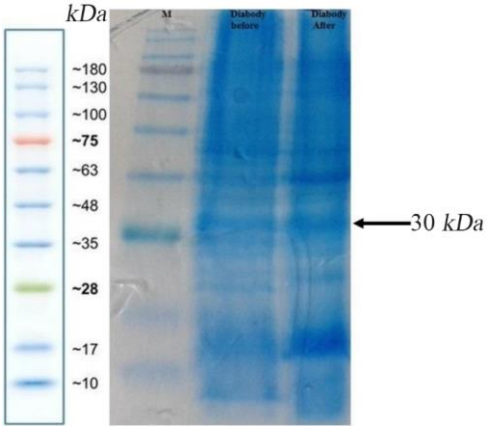

Figure 3. SDS-PAGE analysis of the expressed tandem bivalent anti-VEGF$_{165}$ nanobody showed a band at ~30 *kDa.*

Proliferation assay

The antiproliferative activity of nanobody and tandem bivalent nanobody was studied on HUVEC and HEK293 cells. As expected, the proteins did not exhibit an anti-proliferative activity against HEK293 cells due to lack of VEGFR2 receptor on the surface cell (Data not shown). In contrast, both proteins inhibited the proliferation of HUVEC cells in a dose-dependent manner (Figure 8). Data analysis revealed that there was no significant difference between the antiproliferative activity of tandem bivalent nanobody and the native one.

Pharmacokinetic study

Pharmacokinetic study revealed that the terminal half-life ($T_{1/2}$) increased approximately 2-fold after a

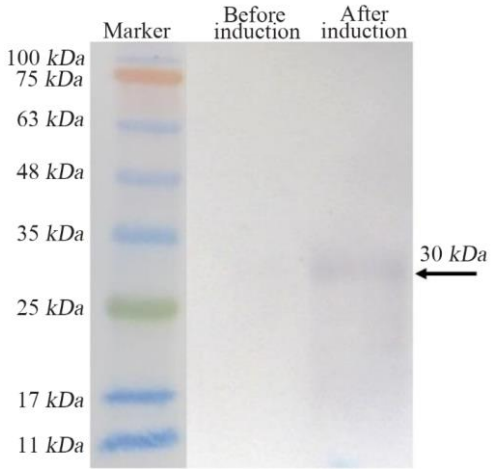

Figure 4. Western blot analysis confiremd the expression of tandem bivalent anti-VEGF$_{165}$ nanobody

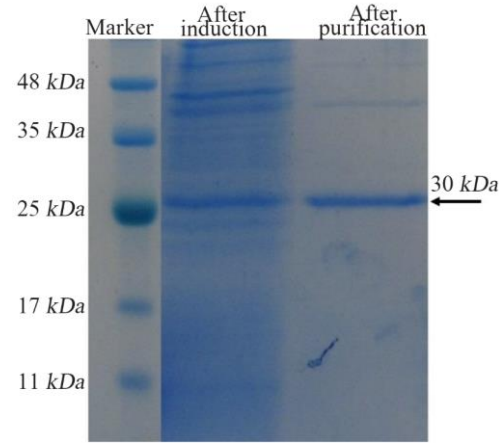

Figure 5. SDS-PAGE analysis of the expressed and purified tandem bivalent anti-VEGF$_{165}$ nanobody showed a band at 30 *kDa*.

Table 1. Size distribution parameters of nanobody and tandem bivalent nanobody

Protein	Average size (d.nm)	PDI	Intensity %
Nanobody	77	0.3	100
Tandem bivalent	153	0.4	100

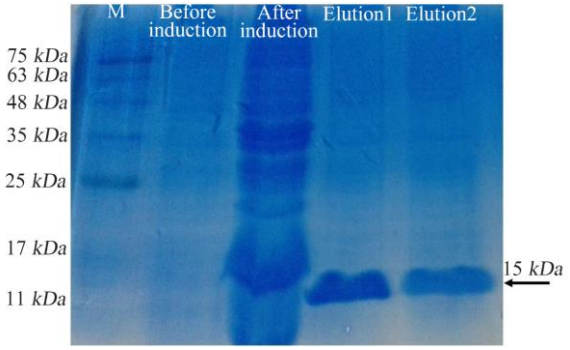

Figure 6. SDS-PAGE analysis of the expressed and purified anti-VEGF$_{165}$ nanobody showed a band at 15 *kDa.*

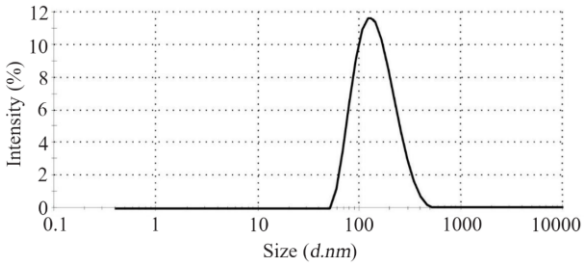

Figure 7. Hydrodynamic radius measuring tandem bivalent anti-VEGF$_{165}$ nanobody using dynamic light scattering.

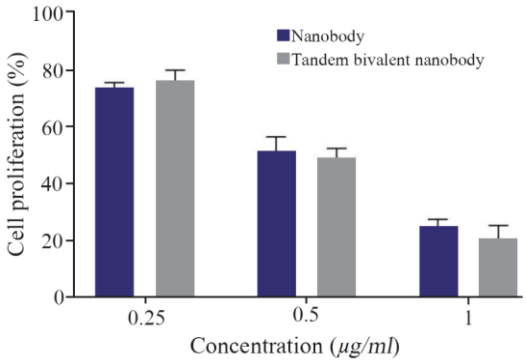

Figure 8. The antiproliferative activity of nanobody and tandem bivalent nanobody on HUVEC cells.

single dose administration of the proteins (Figure 9). The measurement of pharmacokinetic parameters also elucidated that the extended *in vivo* half-life was obtained *via* a decline in the clearance of tandem bivalent nanobody (Table 2).

Discussion

Cancer treatment using monoclonal antibodies is an ongoing practice. Monoclonal antibodies play inevitable roles in medicine and research. Most of them exert their effects by binding to transmembrane receptors or soluble ligands, interfering with signal transduction pathways, and thereby inhibiting tumor cell proliferation and angiogenesis. Because of low stability, solubility, and large size of conventional antibodies, next-generation antibodies have been developed. One approach is development of fragmented antibodies that just contain the antigen binding domain of whole antibodies. However, in some cases, such modifications remarkably affect both the function and affinity of native protein [25,26].

Development of single-domain antibodies with proper antigen-binding specificity is one of the most popular methods for fragmented antibody generation. There is a high sequence similarity between human variable

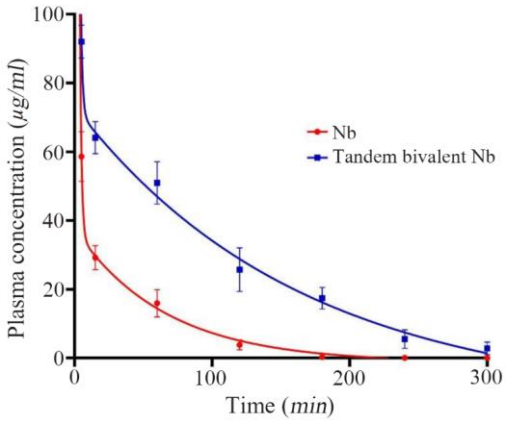

Figure 9. Plasma concentration monitoring of nanobody and tandem bivalent nanobody after injection in mice.

Table 2. Pharmacokinetic parameters obtained for tandem bivalent nanobody and the native one

Protein	$T_{1/2}$ (*min*)	Clearance (*ml/min*)	PK factor
Nanobody	48	0.007	1
Tandem bivalent nanobody	102	0.003	2.1

heavy chains and these fragments. In addition, more hydrophilicity has occurred in these fragments due to four amino acid substitutions in framework 2 that leads to high solubility of such fragmented antibodies [27]. On the other hand, their structure causes high stability and tolerability to hard conditions without losing their biological activity. Despite superior advantages over conventional antibodies, they suffer from low affinity and poor *in vivo* pharmacokinetics [28].

Affinity maturation and multivalency can compensate the low affinity of fragmented antibodies [29]. These miniaturized antibodies also have a short *in vivo* half-life as these small-sized antibodies are rapidly cleared in kidney by glomerular filtration. Some investigations revealed that multivalency could concurrently improve plasma half-life and affinity of nanobodies [30]. Therefore, in the current study, an anti-$VEGF_{165}$ tandem bivalent nanobody was successfully designed, modeled, expressed, and purified to enhance affinity as well as pharmacokinetic parameters of the single domain antibody. The molecular dynamics simulation revealed that the designed nanobody has a good structural stability in water. The purified tandem bivalent nanobody showed a 2-fold increase in the hydrodynamic volume compared to the nanobody. Many studies demonstrated that an increase in the size of small therapeutic proteins could remarkably improve the pharmacokinetic profile *via* a reduction in glomerular filtration rate in kidney [31]. *In vitro* biological activity test elucidated a dose-dependent anti-proliferative activity for nanobody and tandem bivalent nanobody against VEGFR2-expressing HUVEC cells. However, there was no significant difference between the antiproliferative activity of tandem bivalent nanobody and the native one. Moreover, the proteins did not have an anti-proliferative activity against HEK293 cells due to lack of VEGFR2 expression, as also reported in our previous studies [14,23]. The designed tandem bivalent anti-$VEGF_{165}$ nanobody was subjected to further *in vivo* characterization to evaluate the pharmacokinetic enhancement [32,33]. Pharmacokinetic study indicated that the terminal half-life of tandem bivalent nanobody improved approximately 2-fold after an intravenous injection in Balb/c mice. The pharmacokinetic data also revealed that the extended terminal half-life was associated with a decrease in the clearance parameter. In a recent study, Sadeghi A *et al* designed a mono-specific anti-$VEGF_{121}$ bivalent nanobody with extended plasma half-life for treatment of pathologic vascularization [23]. In another study, Behdani *et al* developed an anti-VEGFR2 diabody that could potently inhibit the VEGFR2 receptor on the surface of cancer cells [34].

Conclusion

In conclusion, recent studies indicated that multivalency can improve poor characteristics of fragmented antibodies to generate novel and potent magic tools for cancer therapy.

Acknowledgement

The authors express their deep gratitude to all who provided support during this research.

References

1. Kijanka M, Dorresteijn B, Oliveira S, van Bergen en Henegouwen PM. Nanobody-based cancer therapy of solid tumors. Nanomedicine (Lond) 2015;10(1):161-74.
2. Steeland S, Vandenbroucke RE, Libert C. Nanobodies as therapeutics: big opportunities for small antibodies. Drug Discov Today 2016;21(7):1076-113.
3. Olafsen T, Wu AM. Antibody vectors for imaging. Semin Nucl Med 2010;40(3):167-81.
4. Nelson AL. Antibody fragments: hope and hype. MAbs 2010;2(1):77-83.
5. Gong R, Chen W, Dimitrov DS. Expression, purification, and characterization of engineered antibody CH2 and VH domains. Methods Mol Biol 2012;899:85-102.
6. Reichert JM. Antibodies to watch in 2015. MAbs 2015;7 (1):1-8.
7. Chames P, Van Regenmortel M, Weiss E, Baty D. Therapeutic antibodies: successes, limitations and hopes for the future. Br J Pharmacol 2009;157(2):220-33.
8. Herrington-Symes AP, Farys M, Khalili H, Brocchini S. Antibody fragments: Prolonging circulation half-life special issue-antibody research. Advances in Bioscience and Biotechnology 2013;4(5):689.
9. Fan K, Jiang B, Guan Z, He J, Yang D, Xie N, et al. Fenobody: a ferritin-displayed nanobody with high apparent affinity and half-life extension. Anal Chem 2018; 90(9):5671-7.

10. Cohan RA, Madadkar-Sobhani A, Khanahmad H, Roohvand F, Aghasadeghi MR, Hedayati MH, et al. Design, modeling, expression, and chemoselective PEGylation of a new nanosize cysteine analog of erythropoietin. Int J Nanomedicine 2011;6:1217-27.
11. Maleki A, Madadkar-Sobhani A, Roohvand F, Najafabadi AR, Shafiee A, Khanahmad H, et al. Design, modeling, and expression of erythropoietin cysteine analogs in Pichia pastoris: improvement of mean residence times and in vivo activities through cysteine-specific PEGylation. Eur J Pharm Biopharm 2012;80(3):499-507.
12. Mirzaei H, Kazemi B, Bandehpour M, Shoari A, Asgary V, Ardestani MS, et al. Computational and nonglycosylated systems: a simpler approach for development of nanosized PEGylated proteins. Drug Des Devel Ther 2016;10:1193-200.
13. Khodabakhsh F, Salimian M, Mehdizadeh A, Khosravy MS, Vafabakhsh A, Karami E, et al. New proline, alanine, serine repeat sequence for pharmacokinetic enhancement of anti-VEGF single-domain antibody. J Pharmacol Exp Ther 2020;375(1):69-75.
14. Khodabakhsh F, Norouzian D, Vaziri B, Ahangari Cohan R, Sardari S, Mahboudi F, et al. Development of a novel nano-sized anti-VEGFA nanobody with enhanced physicochemical and pharmacokinetic properties. Artif Cells Nanomed Biotechnol 2018;46(7):1402-14.
15. Morath V, Bolze F, Schlapschy M, Schneider S, Sedlmayer F, Seyfarth K, et al. PASylation of murine leptin leads to extended plasma half-life and enhanced in vivo efficacy. Mol Pharm 2015;12(5):1431-42.
16. Rahbarizadeh F, Ahmadvand D, Sharifzadeh Z. Nanobody; an old concept and new vehicle for immunotargeting. Immunol Invest 2011;40(3):299-338.
17. Dumoulin M, Conrath K, Van Meirhaeghe A, Meersman F, Heremans K, Frenken LG, et al. Single-domain antibody fragments with high conformational stability. Protein Sci 2002;11(3):500-15.
18. Harmsen M, De Haard H. Properties, production, and applications of camelid single-domain antibody fragments. Appl Microbiol Biotechnol 2007;77(1):13-22.
19. Webb B, Sali A. Comparative protein structure modeling using MODELLER. Curr Protoc Bioinformatics 2016;54 (1):5.6. 1-5.6.37.
20. Lovell S, Davis I, Arendall W, de Bakker P, Word J, Prisant M, et al. Structure validation by Calpha geometry: phi, psi and Cbeta deviation. Proteins 2003;50(3): 437-50.
21. Van Der Spoel D, Lindahl E, Hess B, Groenhof G, Mark AE, Berendsen HJ. GROMACS: fast, flexible, and free. J Comput Chem 2005;26(16):1701-18.
22. Humphrey W, Dalke A, Schulten K. VMD: visual molecular dynamics. J Mol Graph 1996;14(1):33-8.
23. Sadeghi A, Behdani M, Muyldermans S, Habibi-Anbouhi M, Kazemi-Lomedasht F. Development of a monospecific anti-VEGF bivalent nanobody with extended plasma half-life for treatment of pathologic neovascularization. Drug Test Anal 2020;12(1):92-100.
24. Liu W, Zhang X, Song C, Bao S, Lai D, Mou J, et al. Expression and characterization of a soluble VEGF receptor 2 protein. Cell Biosci 2014;4(1):14.
25. Skerra A, Pluckthun A. Assembly of a functional immunoglobulin Fv fragment in Escherichia coli. Science 1988;240(4855):1038-41.
26. Fernández LA. Prokaryotic expression of antibodies and affibodies. Curr Opin Biotechnol 2004;15(4):364-73.
27. Vu KB, Ghahroudi MA, Wyns L, Muyldermans S. Comparison of llama VH sequences from conventional and heavy chain antibodies. Mol Immunol 1997;34(16-17):1121-31.
28. Wang X, Campoli M, Ko E, Luo W, Ferrone S. Enhancement of scFv fragment reactivity with target antigens in binding assays following mixing with anti-tag monoclonal antibodies. J Immunol Methods 2004;294(1-2):23-35.
29. Saerens D, Ghassabeh GH, Muyldermans S. Single-domain antibodies as building blocks for novel therapeutics. Curr Opin Pharmacol 2008;8(5):600-8.
30. Plückthun A, Pack P. New protein engineering approaches to multivalent and bispecific antibody fragments. Immunotechnology 1997;3(2):83-105.
31. Kontermann RE. Strategies for extended serum half-life of protein therapeutics. Curr Opin Biotechnol 2011;22 (6):868-76.
32. Coppieters K, Dreier T, Silence K, Haard HD, Lauwereys M, Casteels P, et al. Formatted anti–tumor necrosis factor α VHH proteins derived from camelids show superior potency and targeting to inflamed joints in a murine model of collagen-induced arthritis. Arthritis Rheum 2006;54(6):1856-66.
33. Behdani M, Zeinali S, Khanahmad H, Karimipour M, Asadzadeh N, Azadmanesh K, et al. Generation and characterization of a functional Nanobody against the vascular endothelial growth factor receptor-2; angiogenesis cell receptor. Mol Immunol 2012;50(1-2):35-41.
34. Behdani M, Zeinali S, Karimipour M, Khanahmad H, Asadzadeh N, Azadmanesh K, et al. Expression, purification, and characterization of a diabody against the most important angiogenesis cell receptor: vascular endothelial growth factor receptor 2. Adv Biomed Res 2012;1:34.